

## Intraband relaxation in CdSe quantum dots

Philippe Guyot-Sionnest, Moonsub Shim, Chris Matranga, and Margaret Hines\*

*James Franck Institute, The University of Chicago, 5640 South Ellis Avenue, Chicago, Illinois 60637*

(Received 1 December 1998; revised manuscript received 11 May 1999)

The relaxation of the  $1P$  to  $1S$  electronic states of CdSe semiconductor nanocrystals is followed by infrared pump-probe spectroscopy. Fast (1 ps) and slow ( $>200$  ps) components are observed. Using different capping molecules to control the hole states, we show how the intraband relaxation slows down as the hole is in a shallow trap, a deep trap, or a charge-separated complex, providing strong support for an electron-hole Auger coupling. The slow component corresponds to an energy relaxation rate orders of magnitude slower than in bulk systems. It may be the first indication of the phonon bottleneck effect long expected in strongly confined quantum dots. [S0163-1829(99)51128-4]

A quantum dot is a nanometer-sized semiconductor object that acts much like an artificial atom.<sup>1</sup> The direct relationship between its size and optical properties is generating tremendous interest for a wide variety of optical applications. In particular, it is expected that quantum dots will present superior lasing efficiency over existing quantum-well devices.<sup>2</sup> To date, there has been much progress in the fabrication of quantum dots and even devices but the dynamics of the electronic states in quantum dots remains an open fundamental debate. Electron-phonon coupling is the dominant mechanism for relaxation of electronic states in semiconductors, mostly via longitudinal-optical phonon emission through the Fröhlich coupling in polar crystals. This can lead to very fast energy relaxation rates of the order of  $0.1 \text{ eV ps}^{-1}$ . The problem is that this should be inoperative for strongly confined quantum dots where the electronic energy levels are discrete with spacing far exceeding the phonon energies. The predicted slow relaxation by phonons is called the “phonon bottleneck” effect.<sup>3,4</sup> In contradiction to this prediction, slow intraband relaxations associated with the phonon bottleneck have so far not been seen and fast relaxation is the usual observation.<sup>5-7</sup> Recently, interband optical bleaching experiments of colloidal CdSe quantum dots showed that the bleaching recovery of the second electronic excited state ( $1P$ ) to the first one ( $1S$ ) occurs completely in 300 fs.<sup>8</sup> In highly excited systems, a plausible mechanism involves electron-electron Auger relaxation.<sup>9</sup> For a single electron-hole pair, an Auger-like electron-hole coupling of the electron to the denser manifold of hole states has been proposed.<sup>10</sup> In strongly confined systems with large electron-hole overlap, estimates lead to ps time constants<sup>10</sup> in fair agreement with observations.<sup>8</sup> This process is expected to be weakly temperature dependent, but it should be strongly dependent on the degree of localization of the hole, and it should be eliminated for a quantum dot with no hole.

This paper reports the first intraband study of the relaxation rates of the  $1P$  to  $1S$  electronic states for strongly confined quantum dots. Intraband spectroscopy separates the electron and hole dynamics unlike interband spectroscopies, such as transient visible bleaching or photoluminescence, which automatically involve electron-hole pair. The use of colloidal nanocrystals is motivated by the strong confinement

achievable as well as by the easy surface modifications that allow some control over the hole states.

CdSe colloids are among the best characterized semiconductor quantum dots in the strong confinement regime, and optical absorption shows a rich series of size tunable transitions.<sup>11</sup> A number of models, effective mass,<sup>12</sup> pseudopotentials,<sup>13</sup> and tight binding,<sup>14</sup> have been specifically applied to these systems. The light effective mass of the electron leads to electronic levels that are well described as confined states in a spherical box, and in this work, we discuss transitions from the  $1S$  to the  $1P$  states. These states are split by Coulomb interaction with the hole, distortion from spherical symmetry etc., but the confinement energy (0.3–0.6 eV) is much larger than these perturbations, leading to well-defined intraband transitions.<sup>15</sup> The larger mass and threefold degeneracy of the hole complicate the description of the hole state. The effective-mass approximation with spherical symmetry lead to a delocalized  $S_{3/2}$  wave function for the lowest hole state.<sup>12</sup> This picture is likely to be too ideal. The nanocrystals are strongly polar<sup>16</sup> suggesting rather asymmetric hole wave functions. Se surface dangling bonds are present and hole surface states are expected to be prominent.<sup>17</sup> In addition to the intrinsic surface states, surface capping molecules can introduce localized hole states presenting small overlap with the delocalized interior hole states. Such capping molecules can be exchanged using standard procedure.<sup>18</sup> Trioctylphosphine oxide (TOPO), thiocresol, and pyridine are used here. As discussed below, these three surface treatments weaken the coupling of the hole to the interior states in decreasing order.

The colloidal CdSe nanocrystals are prepared according to established procedures<sup>19</sup> and the data presented are for samples of sizes 3.5 nm (first exciton peak at 545 nm) and 4.3 nm (first exciton peak at 570 nm) with a size dispersion around 8%. The nanocrystals are dispersed in chloroform or heptamethylnonane (a low-temperature glass former) for TOPO and thiocresol treated nanocrystals or solid films of polyvinylbutyral. Pyridine treated nanocrystals are in pyridine solvent. The optical density of the samples at the visible excitation wavelength 532 nm is adjusted between 1 and 2. Liquid samples are 400 microns thick and kept between sapphire windows. Polymer films are dried on a sapphire window.

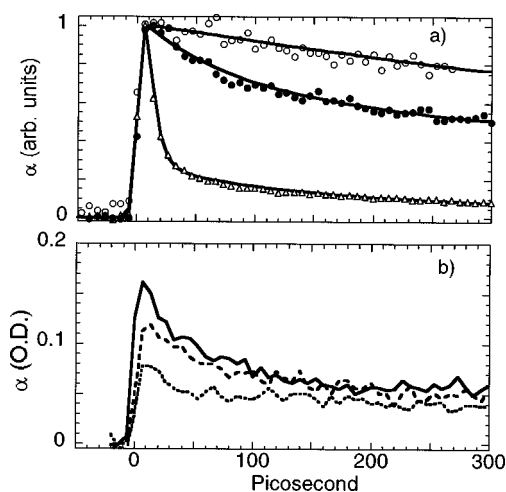


FIG. 1. (a) IR absorbance change  $\alpha$  as a function of delay of the pump visible beam for different surface treatments. TOPO-capped (solid dots) in Paetamethylnonani, thiocresol-capped (open circles) in Paetamethylnonani, and pyridine capped (open triangle) in pyridine, at  $1 \text{ mJ cm}^{-2}$ . (b) IR absorbance change  $\alpha$  for a chloroform solution of thiocresol-capped clusters ( $\text{O.D.}_{532 \text{ nm}} = 0.4$ ) at 1, 3, and  $6 \text{ mJ cm}^{-2}$ . The data exhibit saturation of the electron density of the  $1S$  state as well as an increasingly fast relaxation at an earlier time, attributed to Auger electron-electron interband relaxation.

The optical pulses are derived by various stages of dye laser pumping and parametric mixing from a Nd:YAG (yttrium aluminum garnet) pulsed laser operating at 25 Hz. The transient IR spectroscopy is performed with  $\sim 0.6$  ps pulses tuned to wide transparency ranges of the samples around 3600 and  $2500 \text{ cm}^{-1}$ . These frequencies are close to the peak of the  $1S$ - $1P$  transitions for the two sizes of nanocrystals.<sup>15</sup> The IR beam is split into a pump beam of  $1.5$ – $5 \mu\text{J}$  energy, with a waist  $w_0 = 0.8 \text{ mm}$  corresponding to a peak energy density of  $0.2$ – $0.5 \text{ mJ/cm}^2$ , and a probe beam (about  $50 \text{ nJ}$ ,  $w_0 = 0.2 \text{ mm}$ ). The IR pump beam can be advanced with respect to the probe beam by 100 ps. The visible excitation pulse is a 8 ps, 532-nm beam that is defocused ( $w_0 = 2 \text{ mm}$  with peak energy density adjustable between 0 and  $8 \text{ mJ/cm}^2$ ). The visible pump beam can be advanced by up to 1 ns with respect to the probe IR beam. Changes in the sample absorbance  $\alpha$  are obtained by measuring a reference IR pulse and the transmitted IR pulse with two PbSe photodiodes. With the present setup, the accuracy was limited to about 2% peak to peak over 200 laser shots.

After visible photoexcitation, the electron and the hole relax into their lowest state in less than a picosecond.<sup>8</sup> The lowest delocalized electron state is the  $1S$  state which is directly monitored by the absorption strength of the  $1S$ - $1P$  transition. Decay from the  $1S$  state can occur by nonradiative or radiative recombination with the hole. For multiple electrons, Auger process occurs. Figure 1(a) shows the evolution of the  $1S$ - $1P$  absorption, measured by the probe IR, following the visible beam excitation: Very different results are obtained for TOPO, thiocresol, and pyridine surface modifications.

All three surface modifications passivate the Cd dangling bonds and therefore remove the surface electron traps. However, they do not passivate the surface Se atoms. Calculations indicate that these dangling Se orbitals provide various

surface hole states, mostly shallow traps with deep traps expected only for Se atoms with two lone pairs.<sup>14,17,21</sup> In addition to these intrinsic surface states, the capping molecule can introduce more localized hole states. This is largely in part because from S, N, to O, the electronegativity increases and therefore the ability to trap holes (donate electrons) decreases. TOPO forms a strong complex with Cd via the O lone pair, and with O being very electronegative, TOPO does not introduce specific hole traps. This is why TOPO nanocrystals have strong band-edge emission. Thiophenol adsorbs as thiolates and forms a covalent CdS bond,<sup>20</sup> removing the Cd dangling orbital (electron trap) from the gap. Specific to S, the two lone pairs provide deep hole traps, that are similar though probably shallower than the mid gap states calculated for Se surface atoms.<sup>21</sup> This explains the absence of band-edge fluorescence and the broad shifted emission. These sulfur deep traps must be less coupled to the interior states than the intrinsic shallow Se surface states. With pyridine, the bonding is by complexation of Cd with the lone pair of nitrogen. N is slightly more electronegative than S and does not present nonbonding lone pairs, however the  $\pi$  ring provides additional stabilization for a positive charge, such that, in addition to the intrinsic Se surface states, the photoexcited hole can also be stabilized on pyridine in a charge-separated complex. Nonradiative recombination is ultimately favored and the fluorescence is less than 0.05%. The hole in this charge-separated complex is expected to be weakly coupled to the interior states or to the Se surface states. Our experiment probes the clusters with a long-lived electron in the  $1S$  state and thus preferentially the more stable charge-separated complexes. In Fig. 1(a), after 100 ps, these complexes represent about 20% of the photoexcited nanocrystals. For all three surface modifications, the description above is the expected dominant behavior, shallow Se hole traps for TOPO, deep S hole traps for thiocresol and charge-separated complex for pyridine. However, ensembles of nanocrystals will show overlapping behaviors due to their imperfections.

The  $1S$ - $1P$  absorption also provides a measure of the number of electrons in the  $1S$  state. At low visible pump energy density (below about  $1 \text{ mJ cm}^{-2}$  corresponding to cross sections of  $3 \times 10^{-16} \text{ cm}^2$  at 532 nm, as expected for these samples), only one electron-hole pair is initially created. At higher visible pump energy density, several electrons can be loaded into the  $1S$  state. Figure 1(b) shows how this saturates for higher power. Furthermore, at more than one electron per dot, electron-electron Auger interband relaxation sets in.<sup>22</sup> This depletes the electron density in the  $1S$  state such that after about 200 ps, the dots return in the single electron limit irrespective of the pump energy.

The dynamics of the  $1P$ - $1S$  relaxation are now discussed. With the IR pump energies available, the bleaching signals  $\Delta\alpha/\alpha$  are in the range of 0.2 to 0.6. Such strong bleach signals are expected given the large IR cross section of the  $1S$ - $1P$  transitions. Using the integrated cross section previously measured for these samples,<sup>15</sup> the saturation intensity is expected to be less than  $0.15 \text{ mJ/cm}^2$ . This is an upper limit as we do not yet know the homogeneous linewidths of the transitions. Although the experiments have been performed in the strong saturation regime, complete bleaching was never observed, possibly due to induced absorption to higher electronic states such as  $1P$  to  $1D$  transitions. To

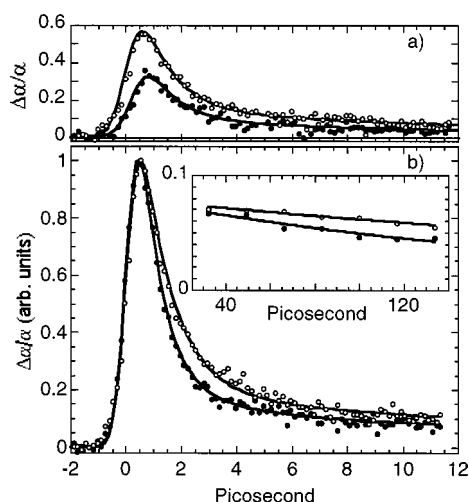


FIG. 2. (a) Bleach decay at 80 K for TOPO-capped nanocrystals in a polyvinylbutyral film with polarization of the IR probe parallel (open dots) and perpendicular (solid dots) with respect to the pump. (b) IR bleach  $\Delta\alpha/\alpha$  at 300 K (solid dots) and 80 K (open dots). The solid lines are multiexponential relaxation from a Gaussian excitation pulse of 0.6 ps full width at half maximum with coefficients of 300 K: (86%, 0.9 ps); (9.5%, 4.3 ps); (4.5%, 200 ps); 80 K: (86%, 1.2 ps); (9.5%, 10 ps); (4.5%, 400 ps). The inset shows the long-time behavior of the bleach decay along with least-square fits exponential behavior of 220 and 410 ps.

check for possible nonlinear effects induced by multiphoton absorption, measurements at higher ( $\times 5$ ) and lower ( $\times 0.2$ ) pump power were performed but the temporal behavior remained essentially identical.

Figure 2(b) shows the transient bleaching for a nanocrystals with peak exciton at 570 nm, with TOPO caps and in a solid film of polyvinylbutyral (1:1 weight ratio) at 300 and 80 K. There is a fast relaxation, as expected from earlier interband studies,<sup>8</sup> but we have also discovered slower components. The fast decays measured here (0.9–1.2 ps) are significantly slower than the 0.3 ps obtained by transient visible bleaching.<sup>8</sup> Visible transient bleaching measurements are inevitably done with a hot hole, while IR intraband measurements done more than 10 ps after the visible pulse allow the hole to cool to its lowest and most localized state.<sup>23</sup> The slower  $1P$ - $1S$  rates observed here are therefore consistent with the electron-hole Auger mechanism. These measurements are not significantly affected by the delay of the IR probe with the green from 30 to 400 ps or by the power of the green indicating that they are representative of the single electron/dot regime. Polarization dependence allows us also to rule out thermal effects. Figure 2(a) shows the bleach signal with the probe polarization parallel and perpendicular to the pump. The bleach polarization ratio is  $(\Delta\alpha/\alpha)_{\parallel}/(\Delta\alpha/\alpha)_{\perp} = 1.8 \pm 0.2$ . A thermal effect would be polarization insensitive in the transmission geometry. Assuming spherical symmetry there should be no bleach signal in the perpendicular pump and probe polarizations. On the other hand, with  $C_{3v}$  symmetry, the bleach polarization ratio for  $A-A$  ( $S$  to  $P_z$ ) or  $A-E$  ( $S$  to  $P_x + iP_y$  or  $P_x - iP_y$ ) transitions are 3 and 4/3, respectively, with an average of 1.88 in accord with the measurement.

The fast energy relaxation rate  $\sim 0.3$  eV ps<sup>-1</sup> is not very different from rates in bulk systems<sup>24</sup> and is not sufficient

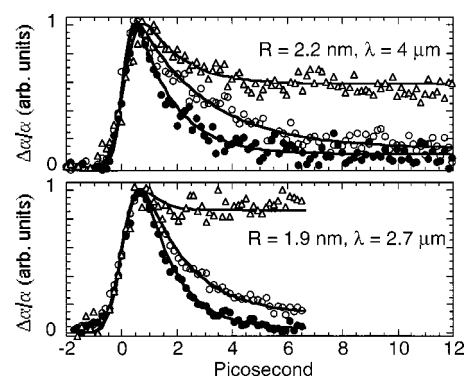


FIG. 3. IR bleach  $\Delta\alpha/\alpha$  for TOPO nanocrystals in heptamethylnonane (solid dots), thiocresol-nanocrystals in heptamethylnonane (open dots), pyridine-nanocrystal in pyridine (open triangles). Two different sizes are shown.

evidence for the electron-hole coupling mechanism.<sup>7</sup> The evidence comes from the systematic effects that different surface caps have on the bleaching relaxation, as shown in Fig. 3. Shallow trapping by Se in TOPO capped dots leads to 1 ps decays instead of the 0.3 ps reported for the hole in its initial photoexcited delocalized state.<sup>8</sup> Deep trapping of the hole by thiocresol further slows down the relaxation by a factor of 2. Charge separation most prominent in pyridine-capped nanocrystals effectively quenches the recombination. The slowing down of the fast relaxation as the hole becomes more decoupled from the interior states, the overall fast rates, and the weak temperature dependence are confirmations of the important role played by holes in the intraband relaxation.

In all samples, the slow relaxation is also observed. While the slow relaxation component is less than 10% of the total bleaching signal for the TOPO or thiol capped samples in solution, it is dominant in pyridine-capped samples. Since we expect pyridine-capped nanocrystals to have the highest propensity for charge separation, we assign this ubiquitous slow relaxation to nanocrystals having undergone charge separation, in agreement with a quenching of the electron-hole Auger coupling. As shown in Fig. 2, this 0.3–0.5 eV energy relaxation is slower than 200 ps at room temperature corresponding to an energy relaxation rate of  $10^{-3}$  eV ps<sup>-1</sup>, or two orders of magnitude slower than in similar bulk systems. This is the slowest intraband relaxation reported in strongly confined quantum dots. Ultimately, the relaxation may be due to multiphonon processes or to coupling to defects as proposed by Sercel.<sup>25</sup> As shown in the inset of Fig. 2(b), cooling to 80 K in thin films of polyvinylbutyral/TOPO nanocrystals leads to an increase of the slow relaxation time but both mechanisms are expected to have some temperature dependence and they are not separated in this work. Experiments along the lines that have been described here, but extended to longer times, lower temperature, and core/shell inorganic structures, will provide definitive answers to the long debate regarding the relaxation of electronic states in quantum dots.

In summary, we demonstrated how transient infrared absorption measurement of the intraband  $1S$ - $1P$  electronic transition in quantum dots can be used to study intraband relaxation in the one electron and one hole or just one-electron limit. We showed how chemical modifications of

the surface of the nanocrystal could be used to modify the coupling of the electron with the hole. The slowing down of the intraband relaxation resulting from hole trapping strongly reinforces the interpretation of previous interband studies<sup>8</sup> which assigned fast ( $<1$  ps) intraband relaxation rates to an electron-hole Auger process.<sup>10</sup> We also discovered a very slow relaxation component ( $>200$  ps) which we assigned to charge-separated quantum dots. This is best shown for pyridine-capped nanocrystals. This slow energy relaxation rate ( $<meV ps^{-1}$ ) is two orders of magnitude slower than in bulk systems, and may be among the first indications for the phonon bottleneck long expected in quantum dots. Transient

infrared intraband studies of colloidal quantum dots along the same line as presented here will also offer a new way to address important issues on quantum dots, in general, as well as on the carrier transfer mechanisms from dot to solution species, surfaces, or other colloids.

This work was funded by the National Foundation under Grant No. DMR-9731642. We made use of the shared MR-SEC Shared Facilities supported by the National Science Foundation under Grant No. DMR-9400379. P.G.S. gratefully acknowledges financial support from the Alfred P. Sloan Foundation.

\*Present address: Revlon, Research Center, 2121 Route 27, Edison, NJ 08818.

<sup>1</sup>M. A. Kastner, *Phys. Today* **46** (1), 24 (1993).

<sup>2</sup>Y. Arakawa and H. Sasaki, *Appl. Phys. Lett.* **40**, 939 (1982).

<sup>3</sup>U. Bockelmann and G. Bastard, *Phys. Rev. B* **42**, 8947 (1990).

<sup>4</sup>H. Benisty, C. M. Sotomayor-Torres, and C. Weisbuch, *Phys. Rev. B* **44**, 10 945 (1991).

<sup>5</sup>G. Wang, S. Fafard, D. Leonard, J. E. Bowers, J. L. Merz, and P. M. Petroff, *Appl. Phys. Lett.* **64**, 2815 (1994).

<sup>6</sup>S. Grosse, J. H. H. Sandmann, G. Vongplessed, J. Feldmann, H. Lipsanen, M. Sopenan, J. Tulkki, and J. Ahopelto, *Phys. Rev. B* **55**, 4473 (1997).

<sup>7</sup>D. Gammon, E. S. Snow, B. V. Shanabrook, D. S. Katzer, and D. Park, *Science* **273**, 87 (1996).

<sup>8</sup>V. Klimov and D. McBranch, *Phys. Rev. Lett.* **80**, 4028 (1998).

<sup>9</sup>U. Bockelmann and T. Egler, *Phys. Rev. B* **46**, 15 574 (1992).

<sup>10</sup>A. L. Efros, V. A. Kharchenko, and M. Rosen, *Solid State Commun.* **93**, 281 (1995).

<sup>11</sup>D. J. Norris and M. G. Bawendi, *Phys. Rev. B* **53**, 16 338 (1996).

<sup>12</sup>A. I. Ekimov, F. Hache, M. C. Schanne-Klein, D. Ricard, C. Flytzanis, I. A. Kurdryavtsev, T. V. Yazeva, A. V. Rodina, and A. L. Efros, *J. Opt. Soc. Am. B* **10**, 100 (1993).

<sup>13</sup>L. W. Wang and A. Zunger, *Phys. Rev. B* **53**, 9579 (1996).

<sup>14</sup>K. Leung, S. Pokrant, and K. B. Whaley, *Phys. Rev. B* **57**, 12 291 (1998).

<sup>15</sup>P. Guyot-Sionnest and M. A. Hines, *Appl. Phys. Lett.* **72**, 686 (1998).

<sup>16</sup>S. A. Blanton, R. L. Leheny, M. A. Hines, and P. Guyot-Sionnest, *Phys. Rev. Lett.* **79**, 865 (1997).

<sup>17</sup>K. Leung and K. B. Whaley, *J. Chem. Phys.* **110**, 1102 (1999).

<sup>18</sup>M. Kuno, J. K. Lee, D. O. Dabbousi, F. V. Mikulec, and M. G. Bawendi, *J. Chem. Phys.* **106**, 9869 (1997).

<sup>19</sup>C. B. Murray, D. J. Norris, and M. G. Bawendi, *J. Am. Chem. Soc.* **115**, 8706 (1993).

<sup>20</sup>I. G. Dance, A. Choy, and M. L. Scudder, *J. Am. Chem. Soc.* **106**, 6285 (1984).

<sup>21</sup>S. Pokrant and K. B. Whaley, *Eur. Phys. J. D* **6**, 255 (1999).

<sup>22</sup>V. L. Klimov and D. W. McBranch, *Phys. Rev. B* **55**, 13 173 (1997).

<sup>23</sup>V. Klimov, P. Haring Bolivar, and H. Kurz, *Phys. Rev. B* **53**, 1463 (1996).

<sup>24</sup>V. Klimov, P. Haring Bolivar, and H. Kurz, *Phys. Rev. B* **52**, 4728 (1995).

<sup>25</sup>P. C. Sercel, *Phys. Rev. B* **51**, 14 532 (1995).